



Published in final edited form as:

*Nat Neurosci.* 2012 September ; 15(9): 1313–1319. doi:10.1038/nn.3186.

## Olfactory input is critical for sustaining odor quality codes in human orbitofrontal cortex

Keng Nei Wu<sup>1</sup>, Bruce K. Tan<sup>2</sup>, James D. Howard<sup>1</sup>, David B. Conley<sup>2</sup>, and Jay A. Gottfried<sup>1,3,4</sup>

<sup>1</sup>Department of Neurology, Northwestern University, Chicago, IL, USA

<sup>2</sup>Department of Otolaryngology - Head and Neck Surgery, Northwestern University, Chicago, IL, USA

<sup>3</sup>Cognitive Neurology & Alzheimer's Disease Center, Feinberg School of Medicine, Northwestern University, Chicago, IL, USA

<sup>4</sup>Department of Psychology, Northwestern University Weinberg College of Arts and Sciences, Evanston, IL, USA

### Abstract

Ongoing sensory input is critical for shaping internal representations of the external world. Conversely, a lack of sensory input can profoundly perturb the formation of these representations. The olfactory system is particularly vulnerable to sensory deprivation, due to the widespread prevalence of allergic, viral, and chronic rhinosinusitis, but how the brain encodes and maintains odor information under such circumstances remains poorly understood. Here we combined functional magnetic resonance imaging (fMRI) with multivariate (pattern-based) analyses and psychophysical approaches to show that a seven-day period of olfactory deprivation induces reversible changes in odor-evoked fMRI activity in piriform cortex and orbitofrontal cortex (OFC). Notably, multivoxel ensemble codes of odor quality in OFC became decorrelated following deprivation, and the magnitude of these changes predicted subsequent olfactory perceptual plasticity. Our findings suggest that transient changes in these key olfactory brain regions are instrumental in sustaining odor perception integrity in the wake of disrupted sensory input.

---

In the 1960s, a series of landmark studies on the visual system of the developing cat highlighted the importance of sensory experience in shaping brain organization and function<sup>1</sup>. This work, along with studies of neural remapping of rodent barrel cortex<sup>2</sup> and monkey somatosensory cortex<sup>3</sup>, provided a powerful neuroscientific foundation that remains highly influential for understanding sensory system processing. A fundamental implication

---

Users may view, print, copy, download and text and data- mine the content in such documents, for the purposes of academic research, subject always to the full Conditions of use: [http://www.nature.com/authors/editorial\\_policies/license.html#terms](http://www.nature.com/authors/editorial_policies/license.html#terms)

#### Author contributions

J.A.G. conceived the experiment, with extensive contributions and methodological suggestions from K.N.W., D.B.C., and J.D.H. K.N.W. collected the imaging and behavioral data. D.B.C. and B.K.T. collected and analyzed the nasal endoscopy and rhinometry data. K.N.W. analyzed the behavioral and imaging data with assistance from J.D.H. and J.A.G. K.N.W., J.D.H., and J.A.G. wrote the manuscript.

is that our sensory systems are not mere passive receivers of information, but active respondents. It is the complex interaction between stimulus input and individual experience that defines the form and function of the brain, and ultimately how sensory systems perceive and respond to the external environment.

These earlier studies introduced the concept of the “critical period”, a time-limited window in an organism’s early development during which there is particularly robust plasticity in response to sensory experience<sup>4</sup>. However, closure of the critical window does not mean shutting the door to sensory-driven plasticity<sup>5–8</sup>. Periods of sensory deprivation later in life can alter brain activity and function, albeit in less dramatic ways than during development<sup>9–14</sup>. Several studies have demonstrated sensory behavioral plasticity resulting from short-term visual, auditory, and somatosensory deprivation in adult humans<sup>15–19</sup>. Some of this work has also demonstrated measurable changes in brain activity as a result of sensory deprivation, including visual cortex excitability<sup>15,16</sup>, cross-modal neuroplasticity<sup>20</sup>, and response tuning shifts in the adult human auditory<sup>17</sup> and somatosensory<sup>18</sup> cortex. Such observations suggest that consistent ongoing afferent input may be important in maintaining the integrity of sensory systems throughout life.

The olfactory system presents an especially interesting case for the studying of perceptual plasticity due to its highly regenerative nature. Olfactory sensory neurons (OSNs) are continuously regenerated and replaced throughout life<sup>21,22</sup>, and the olfactory bulb is one of the only sites in the human brain to be replenished with new neurons throughout the lifespan<sup>14,23</sup>. Recent studies have shown that the human olfactory system remains highly pliable into adulthood. For example, previous work in our laboratory has shown that brief passive exposure to an odor, as well as associative conditioning between an odor and footshock, is sufficient to induce perceptual and neural enhancement of olfactory discrimination<sup>7,8</sup>. Such findings illustrate the key role of afferent sensory experience in optimizing olfactory system function.

The corollary – that a lack of sensory experience might have a detrimental impact on olfactory processing – has been explored in rodent models. These studies have helped elucidate basic operations of the olfactory system, as well as mechanisms underlying sensory plasticity. One widely employed method of inducing olfactory deprivation is unilateral nostril (naris) occlusion. Both anatomical and neurochemical changes have been identified in the rodent olfactory bulb (OB) and even in primary olfactory cortex using this technique<sup>10–13,24–29</sup>. Following unilateral naris occlusion, an overall increase in odor-evoked metabolic activity in the OB glomerular layer occurred alongside a decrease in the stimulus specificity of odor-evoked single-unit responses in mitral/tufted cells<sup>25</sup>. Notably, despite dramatic physiological changes, odor deprivation often has no effect on olfactory behavior<sup>26</sup>, and paradoxically sometimes enhances detection and discrimination performance when compared to control rats<sup>24</sup>. The fact that a unilaterally occluded OB can still gain odor access via a septal “window” between the nasal chambers<sup>30</sup>, and that unilateral inputs may nevertheless activate higher-order centrifugal projections bilaterally<sup>31</sup>, may account for these mixed findings. A more ideal procedure would be to occlude both nostrils simultaneously, but this approach is unfeasible in obligatory nose breathers such as rodents.

To date, there have been no studies investigating the effects of olfactory deprivation in humans. The impracticality of bilateral nostril occlusion in rodents, as noted above, can be overcome in humans, whose respiratory anatomy permits bilateral odor deprivation. Here we introduce a novel method of odor deprivation in human subjects, in combination with psychophysical measurements, functional magnetic resonance imaging (fMRI), and multivariate (pattern-based) imaging analysis, to assess how a seven-day absence of odor afferent input modulates olfactory perceptual representations in the human brain. This design enabled us to test two specific hypotheses that were motivated from prior animal findings<sup>25</sup>. First, we asked whether odor deprivation would induce general gains in overall response sensitivity to odor stimuli as indexed via perceptual thresholds and fMRI activity in central olfactory brain areas. This was the main aim of fMRI Experiment 1. Second, we asked whether olfactory afferent input is necessary to sustain the specificity of categorical representations of odor object quality, as reflected in odor discriminability and spatial patterns of odor-evoked fMRI activity in the human olfactory system. This was the main aim of fMRI Experiment 2.

## Results

The total length of the experiment spanned two weeks (Fig. 1a), involving a one-week period of odor deprivation and a one-week recovery period. On day 0, subjects underwent baseline psychophysical testing and olfactory fMRI scanning. They were subsequently admitted to the Clinical Research Unit at Northwestern Memorial Hospital for seven days of odor deprivation, during which time their nostrils were occluded with foam tape during waking hours.

Psychophysical tests and fMRI scanning sessions were repeated immediately following odor deprivation (day 7) and again after recovery (day 14). Note that findings were considered “deprivation-specific” only if the changes from pre- to post-deprivation also returned to baseline levels at recovery, thereby minimizing potential confounds related to training effects or mere exposure across the multiple testing days.

### Intranasal anatomy and odor perception

The possibility that seven days of odor deprivation could induce nasal congestion or inflammation, with possible compromise of airflow and peripheral olfactory function, was carefully assessed throughout the study. On days 0, 6, 7, and 14, subjects underwent nasal endoscopy and acoustic rhinometry by trained ENT physicians (Fig. 2). Qualitative endoscopic assessments of the nasal cavity revealed no major instances of edema, discharge, scarring, or crusting. Quantitative endoscopic and acoustic rhinometric measurements revealed no significant change in the space between the inferior turbinate and septum ( $F_{1,99,19,90} = 0.56$ ,  $P = 0.58$ ,  $n = 11$ ; Fig. 2e), or between the middle turbinate and septum ( $F_{1,50,14,97} = 0.13$ ,  $P = 0.82$ ; Fig. 2f). The volume of the nasal cavity (1–5 cm from the entrance of the naris) also remained stable over testing days ( $F_{2,19,19,73} = 0.18$ ,  $P = 0.86$ ,  $n = 10$ ; Fig. 2g). These results suggest that peripheral changes in nasal anatomy were unlikely to have influenced the behavioral and neuroimaging findings.

Behavioral analysis revealed that the one-week deprivation period had no major impact on olfactory function, with regard to either odor detection or discrimination. Apart from the smell identification task (UPSIT) ( $F_{1,81,23,54} = 3.62$ ,  $P = 0.047$ ), psychophysical task performance remained constant over all testing sessions (Table 1). Participants improved significantly on the UPSIT from pre- to post-deprivation ( $T_{13} = 2.39$ ,  $P = 0.033$ ), though the effect was small (3.6% improvement). However, because performance at recovery did not return to baseline levels, this change may have reflected a practice effect. These null results are consistent with rodent studies demonstrating minimal behavioral alterations following even longer periods of naris occlusion<sup>24,26</sup>, suggesting that the adult olfactory system may compensate for diminished afferent odor input via functional plasticity. Whether deprivation induces plasticity in olfactory brain regions, despite preserved perceptual performance, motivated our subsequent imaging analyses.

### Exp. 1: Deprivation-induced mean changes in fMRI activity

During each time-point (day 0, baseline; day 7, post-deprivation; day 14, recovery), subjects took part in two fMRI experiments. Experiment 1, a simple odor detection task (Fig. 1b; Supplementary Fig. 1a), assessed whether odor deprivation had a reversible modulatory effect on stimulus-evoked mean fMRI signal in olfactory-related brain areas. Complete neuroimaging data for this task were obtained from 10 subjects. Detection accuracy was high across all three testing sessions (odor trials:  $96.9\% \pm 1.33$ , mean  $\pm$  S.E.M.; no-odor trials:  $86.4\% \pm 3.63$ ). Importantly, accuracy did not significantly differ across sessions, indicating that any deprivation-related changes in fMRI activity could not be attributed to poor or variable performance across days (odor trials:  $F_{1,47,13,27} = 2.12$ ,  $P = 0.17$ ; no-odor trials:  $F_{1,51,13,59} = 0.34$ ,  $P = 0.66$ ). Similarly, there were no significant respiratory differences in sniff volume ( $F_{1,32,7,89} = 2.44$ ,  $P = 0.16$ ,  $n = 7$ ) or duration ( $F_{1,20,7,18} = 3.15$ ,  $P = 0.12$ ) across testing periods (Supplementary Fig. 2).

We first asked whether mean odor-evoked activity in olfactory brain regions differed across baseline, post-deprivation, and recovery. A one-way repeated-measure ANOVA identified significant time-dependent changes in right anterior piriform cortex (APC), bilateral posterior piriform cortex (PPC), bilateral orbitofrontal cortex (OFC), and bilateral anterior insula (Fig. 3a; Supplementary Table 1). To establish that these activation differences were specific to odor deprivation, and not due to mere factors such as the passage of time or increased task familiarity over the 14-day period, we tested whether response profiles in these brain areas showed a selective decrease in odor-evoked activity as a consequence of deprivation, returning towards baseline levels at recovery. These effects were examined by testing the conjunction of two contrasts: [baseline>post-deprivation] and [recovery>post-deprivation]. We found that the left PPC ( $-14, -2, -18$ ) showed a deprivation-related decline in odor-evoked activity that recovered to baseline at the time of the day 14 scan (Fig. 3b). Note that significant differences were observed when each contrast component of the conjunction analysis was tested separately (baseline>post-deprivation:  $T_9 = 3.23$ ,  $P = 0.002$  uncorrected [unc.]; recovery>post-deprivation:  $T_9 = 2.90$ ,  $P = 0.004$  unc.), confirming the robustness of these effects.

It is equally possible that the deprivation procedure might have induced *selective increases* in odor-evoked activity. Therefore, we also tested the conjunction<sup>32,33</sup> of [post-deprivation>baseline] and [post-deprivation>recovery], which identified areas in the anterior and posterior OFC corresponding to Walker's area 11 (16, 44, -16) and area 13 (16, 16, -18; and -20, 14, -16), respectively (Fig. 3d,f). These response enhancements were transient, returning to baseline levels after the recovery period. Again, separate analyses of the individual contrast effects were significant for post-deprivation>baseline (right anterior OFC,  $T_9 = 4.21$ ,  $P < 0.001$  unc.; right posterior OFC,  $T_9 = 3.63$ ,  $P < 0.001$  unc.; left posterior OFC,  $T_9 = 3.19$ ,  $P < 0.002$  unc.) and for post deprivation>recovery (right anterior OFC,  $T_9 = 3.93$ ,  $P < 0.001$  unc.; right posterior OFC,  $T_9 = 3.77$ ,  $P < 0.001$  unc.; left posterior OFC,  $T_9 = 2.90$ ,  $P < 0.004$  unc.), suggesting that these findings were not preferentially driven by either contrast.

Finally, to assess the statistical robustness of these imaging effects, we conducted a leave-one-subject-out analysis<sup>34</sup> to establish an independent method of voxel selection for purposes of small-volume correction<sup>35</sup>. Values extracted via this method were tested for differences over time and were still significant for all three regions identified in the conjunction analyses, including left PPC ( $F_{1,20,10.77} = 11.61$ ,  $P = 0.005$ ), right anterior OFC ( $F_{1,14,10.27} = 13.58$ ,  $P = 0.003$ ), and right posterior OFC ( $F_{1,89,17.01} = 13.73$ ,  $P = 0.0003$ ) (Fig. 3c,e,g; Supplementary Table 2). Of note, deprivation had no impact on the mean fMRI signal change in APC ( $P > 0.1$ , unc.). That odor deprivation had a regionally selective impact on PPC and OFC, but not on APC, suggests that the hospital environment or other treatment parameters did not have a generalized, non-specific effect on olfactory coding from pre- to post-deprivation.

## Exp. 2: deprivation-induced pattern changes in OFC

Having established that olfactory deprivation has an overall effect on odor-evoked response magnitudes in PPC and OFC, we next asked if the reduction in afferent sensory input has a direct impact on odor quality representations in these areas. To this end, the main objective of fMRI Experiment 2 was to investigate whether odor-specific patterns of ensemble brain activity were degraded following deprivation. Subjects were presented with four different odor stimuli that systematically varied in odor perceptual quality and molecular functional group<sup>8</sup>, and the task was to judge whether odor was present or absent on each trial (Fig 1b; Supplementary Fig. 1b). Complete neuroimaging data for this task were obtained from 11 subjects.

Perceptual ratings obtained outside the scanner confirmed that odorant pairs belonging to the same perceptual category were rated more alike than pairs belonging to different categories ( $T_{12} = 4.29$ ,  $P = 0.001$ ). These effects remained stable across all three sessions (same quality,  $F_{1,63,19.54} = 0.67$ ,  $p = 0.50$ ; different quality,  $F_{1,75,20.97} = 0.12$ ,  $P = 0.86$ ; Fig. 4a). Moreover, behavioral ratings of the odorants did not significantly differ in odor intensity ( $F_{1,51,19.64} = 0.98$ ,  $P = 0.37$ ), pleasantness ( $F_{1,61,20.87} = 1.33$ ,  $P = 0.28$ ), or familiarity ( $F_{1,40,18.23} = 0.98$ ,  $P = 0.37$ ) over test sessions. Performance during scanning again demonstrated high detection accuracy (odor trials:  $91.03\% \pm 3.30$ ; no-odor trials:  $90.8\% \pm 2.34$ ) and remained stable through baseline, post-deprivation, and recovery ( $F_{1,34,14.79} =$

1.63,  $P = 0.23$ ). There were also no odor-evoked differences in sniff inspiratory volume ( $F_{1,94,17.45} = 2.28$ ,  $P = 0.13$ ;  $n = 10$ ) or duration ( $F_{1,25,11.26} = 0.16$ ,  $P = 0.75$ ) across scanning days that might have confounded the imaging analysis (Supplementary Fig. 3).

We took advantage of the fact that the odor stimuli used in this task systematically differed in perceptual quality to explicitly test whether olfactory categorical representations were altered following deprivation. In a multivariate fMRI analysis, odor-specific voxel-wise activity patterns were extracted from APC, PPC, and OFC, and pairwise correlations between odors were calculated. Here the prediction was that at baseline (Day 0), odor-evoked ensemble patterns of fMRI activity would exhibit greater overlap (i.e., be more strongly correlated) for odorants *similar* in quality (e.g., peppermint and spearmint) than for odorants different in quality (e.g., peppermint and rose), and that these odor quality-specific effects would be disrupted after deprivation (Day 7). As with the results reported previously, we only considered effects to be attributable specifically to deprivation if they returned to baseline levels at recovery (day 14).

To test these predictions, linear correlations were calculated between fMRI activity patterns evoked by odorant pairs similar in quality, and compared to correlations between patterns evoked by odorant pairs that differed in quality. Among the olfactory ROIs, a deprivation-specific effect was found only in OFC, exhibiting pattern decorrelation, or divergence, in odor categorical discrimination (main effect of day:  $F_{1,91,19.08} = 8.97$ ,  $P = 0.002$ ; baseline > post-depriv.:  $T_{10} = 3.47$ ,  $P = 0.006$ ; recovery > post-depriv.:  $T_{10} = 3.51$ ,  $P = 0.006$ ) (Fig. 4b). A complementary analysis of odorant pairs similar (vs. different) in molecular functional group did not reveal significant deprivation-related pattern changes in APC, PPC, or OFC.

We also tested whether odor deprivation had a general effect on olfactory coding patterns, irrespective of quality or functional-group membership. This approach revealed that in APC, odor-evoked ensemble patterns of activity became decorrelated after deprivation, returning to baseline levels at recovery ( $F_{1,41,14.05} = 4.93$ ,  $p = 0.033$ ; baseline>post,  $T_{10} = 2.92$ ,  $p = 0.015$ ; recovery>post,  $T_{10} = 3.00$ ,  $p = 0.013$ ; Fig. 5a). Similar trends were observed in the PPC ( $F_{1,34,13.38} = 3.38$ ,  $p = 0.079$ ; post>pre,  $T_{10} = 3.40$ ,  $p = 0.007$ , recovery>post,  $T_{10} = 2.22$ ,  $p = 0.051$ ; Fig. 5b) and OFC ( $F_{1,77,17.67} = 3.68$ ,  $p = 0.051$ ; post>baseline,  $T_{10} = 2.30$ ,  $p = 0.044$ ; recovery>post,  $T_{10} = 2.41$ ,  $p = 0.037$ ; Fig. 5c) but not in the putamen ( $F_{1,99,19.92} = 1.414$ ,  $p = 0.266$ ; Fig. 5d), a non-olfactory control ROI. In fact, direct statistical comparison between the pattern effects in the olfactory ROIs and the putamen (baseline vs. post-deprivation) demonstrated significant differences in all three olfactory regions, including APC ( $T_{10} = -3.82$ ,  $p = 0.003$ ), PPC ( $T_{10} = -3.92$ ,  $p = 0.003$ ), and OFC ( $T_{10} = -3.21$ ,  $p = 0.009$ ), suggesting that deprivation-induced pattern decorrelation was relatively specific to the olfactory system.

### Correlations between brain and behavior

Although the odor deprivation procedure had no overt group effect on behavior, it remains possible that the magnitude of deprivation-induced fMRI plasticity might still predict alterations in olfactory perception, on a subject-by-subject basis. In particular, given that human PPC and OFC have both been implicated in experience-dependent plasticity and odor



quality coding<sup>7,8,36</sup>, we tested whether subject-wise changes in fMRI activity from pre- to post-deprivation correlated with behavioral changes in odor similarity ratings (as an index of odor categorical perception). These analyses were conducted by regressing similarity ratings either against fMRI changes in mean activity levels (cf. Fig. 3) or against fMRI changes in ensemble pattern coherence (cf. Fig. 4). Notably, subject-wise behavioral changes in perceptual similarity ratings were systematically associated only with the degree of odor quality-related pattern decorrelation in OFC (Spearman  $\rho = 0.64$ ,  $P = 0.044$ ,  $n = 10$ ) (Fig. 4c). Thus, with greater disruption of odor quality categorization in OFC, there was a greater corresponding difficulty being able to perceive categorical differences between the odorants.

### Control analyses

Given the odor-evoked increase in mean OFC sensitivity after deprivation (Fig. 3d-g), the OFC pattern decorrelation (Fig. 4) could theoretically be accounted for by fMRI signal saturation. This would result in fMRI patterns across voxels exhibiting weaker category discriminability, with consequent pattern decorrelation. Several control analyses (Supplementary Figure 4) indicated that such mechanisms were not likely to contribute to the deprivation-related pattern changes in OFC activity. Moreover, the mean fMRI signal change in OFC following deprivation (Fig. 3) was  $\sim 0.05$ – $0.06\%$ , well within the range of previous reports demonstrating OFC percent signal change of up to  $0.5\%$ <sup>37,38</sup>.

Finally, in that odorants typically contain trigeminal components, it is possible that trigeminal stimulation per se could have influenced the findings. For example, among the four odorants used in fMRI experiment 2 (odor discrimination), the two minty odorants are known to stimulate the trigeminal nerve and elicit cooling sensations, and it is unclear whether this could impact on our observations. A complementary analysis of the fMRI dataset from experiment 2 revealed that this was unlikely to be the case (Supplementary Figure 5).

### Discussion

How a sustained interruption of odor input affects the human olfactory system has not been previously tested. In this study, we developed a method to induce prolonged odor deprivation in humans, while concurrently minimizing inadvertent exposure to incidental smells. A combination of psychophysical testing, olfactory fMRI, and multivariate pattern analysis enabled us to examine olfactory system responsiveness to a seven-day disruption of sensory stimulation.

Data collection at baseline, post-deprivation, and recovery sessions allowed us to assess changes over time. Behaviorally our findings demonstrate that the olfactory system is able to maintain olfactory perceptual performance despite a substantial reduction in odor afferent input. In parallel, the deprivation procedure elicited reversible changes in piriform and orbitofrontal cortices that may be instrumental in sustaining odor perception in the wake of disrupted input.

It is interesting that deprivation selectively influenced odor quality coding in OFC, a higher-order processing regions, rather than in olfactory sensory regions per se. Multivariate

analysis of the odor quality data (Fig. 5a) showed that at baseline, ensemble patterns in OFC correlated more strongly for odorants belonging to the same category than for odorants belonging to different categories. Following deprivation, these pattern-based perceptual representations became decorrelated, such that qualitatively similar odorants were no longer encoded as members of the same odor object category. Insofar as PPC and OFC are interconnected in both rodents<sup>39,40</sup> and monkeys<sup>41</sup>, the reciprocal response changes after deprivation – a mean *decrease* in PPC and a mean *increase* in OFC (Fig. 3) – may arise from functional interactions between these two regions to optimize olfactory perception after a period of reduced odor input.

Few animal studies have investigated the effects of odor deprivation beyond the olfactory bulb. Although deprivation-induced changes in odor-evoked cortical representations have been described in rodent APC and PPC<sup>13,28</sup>, the impact on OFC has not previously been examined. As odor categorical perception relies on linking olfactory inputs with object-knowledge representations, participation of OFC in this process accords with its broader role in linking odor cues with outcome representations in rodent paradigms of olfactory discrimination learning<sup>42–45</sup>. Given the reported role of human OFC in olfactory attention<sup>38,46</sup>, it is also possible that the interruption of odor input (as indexed by reduced PPC activity) places greater demands on OFC to focus attentional resources on the incoming stimulus. That being said, with the known technical limitations of fMRI, our data cannot rule out the potential involvement at the level of the olfactory sensory neurons or bulb. Notably, a prior odor deprivation study in adult rats<sup>13</sup> highlighted neuronal plasticity in associational cortical networks, implying that deprivation may in fact target higher-order sensory processing areas.

Data across the two imaging paradigms highlight an interesting functional dichotomy in OFC as a consequence of deprivation. An overall mean increase in stimulus-evoked activity in OFC would be consistent with an enhancement of response *sensitivity* to odors. In turn, a reduction in the strength of ensemble pattern coding in OFC may indicate a disruption of response *specificity* for odor object categories. This dichotomy is reminiscent of prior rodent data on odor deprivation<sup>25</sup>, in which an increase in odor-evoked metabolic activity in the rodent glomerular layer occurred alongside a decrease in stimulus specificity of odor-evoked single-unit responses in mitral/tufted cells. Although differences in species, experimental protocols, and brain areas distinguish our study from the rodent work, a common theme nevertheless emerges: the olfactory system reacts to a prolonged lack of afferent stimulation with increased responsiveness, but at the expense of decreased discriminability. Ecologically this perceptual recalibration might favor detection of odors in lower concentration ranges while limiting the capacity to make fine-grained judgments between odors.

Given the technical challenges and potential complications involved in occluding airflow through the nostrils for seven days, it was important to rule out important confounds. Nasal endoscopic and acoustic rhinometry measurements confirmed that deprivation had no impact on peripheral intranasal anatomy. Odor intensity and pleasantness ratings, as well as sniffing behavior, remained constant throughout the experiment, making it unlikely that deprivation-related fMRI plasticity could have been driven by these factors. Critically, the use of a within-subjects factorial design enabled us to test the interaction between odor



quality category and time, minimizing confounds related to mere effects of environment or treatment parameters.

Rodent models of odor deprivation have revealed profound morphological and physiological changes in rodent olfactory epithelium and olfactory bulb when ongoing afferent stimulation is compromised<sup>10,11,25,29,47</sup>. Remarkably, most rodent studies of odor deprivation describe minimal behavioral impact on olfactory perception, and our human behavioral data are in line with these observations<sup>24,26</sup>. Nonetheless, the fact that significant behavioral changes were not seen after deprivation still raises the question whether seven days of nostril occlusion in adult humans was sufficient to modulate olfactory system function. Although unilateral naris occlusion in rodents is typically maintained over a duration of several weeks, it is apparent that the effects of deprivation on the olfactory bulb can occur within 24 hours, and even in as little as 15 minutes after naris occlusion<sup>27,48,49</sup>. These observations make it highly conceivable that robust neurophysiological changes could arise from a seven-day deprivation period in the human brain.

We have previously reported that brief exposure to an odor can enhance odor perceptual differentiation, with parallel learning-induced responses in PPC and OFC. Additionally, the magnitude of learning-induced OFC change was predictive of the level of behavioral improvement<sup>8</sup>. Here, we observed the inverse phenomenon: after a period of deprivation of olfactory experience, categorical specificity in the OFC was disrupted, and this change in brain activity pattern was correlated with behavioral changes in quality similarity ratings between odorants. Consistent with previous rodent studies of olfactory deprivation<sup>24,26</sup>, we found changes in brain activity levels and ensemble patterns in putative olfactory regions without measurable behavioral deficits. The fact that odor perception was nominally preserved at the group level suggests that the olfactory system possesses compensatory mechanisms that render it resistant to transient perturbations of afferent sensory input, as commonly occurs during extended instances of rhinosinusitis or upper respiratory infections<sup>50</sup>. Whether the observed changes in mean OFC activity explicitly support odor perception in the wake of impoverished input remains to be established in future studies.

## Methods

### Subjects

We obtained informed consent from 14 subjects (8 women; mean age, 23.8 years) to participate in this study, which was approved by the Northwestern University IRB. Subjects were right-handed non-smokers with no history of significant medical illness, psychiatric disorder, or smell, taste, or ear-nose-throat (ENT) disorder.

### Odor deprivation procedure

After the first scanning session (Day 0), subjects were admitted to the Clinical Research Unit (CRU) at Northwestern Memorial Hospital (NMH) for seven inpatient days (six nights). The odor deprivation technique involved placing Microfoam surgical tape (3M) securely over the nostrils to occlude nasal airflow. Merocel nasal tampons (Medtronic) were cut into 1-cm strips and placed just inside the nostrils at the inner aspect of the tape, to

absorb excess moisture that collected at the entrance to the nose that might loosen the tape seal. The dressing was replaced once every four hours during waking hours or sooner if an air leak was detected. The dressing was removed when subjects went to sleep at night, and a new dressing was applied when they first woke up in the morning, prior to getting out of bed.

There were several important benefits of the CRU. First, an odor-free environment in a negative-pressure room was constantly maintained. Second, a healthy, bland diet designed by CRU dietician was provided to minimize retronasal exposure to odors. Third, fragrance-free room products were used to clean the hospital room, sheets, and towels. Fourth, subjects were provided with fragrance-free toiletries (toothpaste, shampoo, etc.). Fifth, nursing staff were on hand to closely monitor subjects' compliance with odor deprivation and respond quickly to any unexpected airflow breaches through the nasal dressing.

### **Nasal endoscopy and acoustic rhinometry**

These procedures were performed in the ENT Department at NMH on days 0, 6, 7, and 14. The presence of discharge, edema, scarring, or crusting in each nostril was noted during endoscopy. Moreover, the spaces between the inferior turbinate and septum, and between the middle turbinate and septum, were recorded for each nostril. Acoustic rhinometry<sup>51</sup> was used to quantify intranasal volume and cross-sectional area of the nasal cavity. Due to normal physiological variations in nasal cycle<sup>52</sup>, all measurements were averaged across both nostrils. Because one subject showed endoscopic evidence for edema on day 6, this individual remained in the odor-free environment without nostril occlusion for the final 24 hrs, with clinical improvement on day 7. Bilateral intranasal volume at day 7 (2.77 cm<sup>3</sup>) was similar to that measured at baseline (2.87 cm<sup>3</sup>).

### **Odor stimuli**

The four odorants used in the basic odor detection task (fMRI experiment 1) were anisole, butanol,  $\alpha$ -ionone, and heptanal. Four different odorants<sup>8</sup> were used in a separate fMRI assessment of odor categorical perception (fMRI experiment 2), and included two “minty” smells ((*R*)-carvone and L-menthol) and two “floral” smells (acetophenone and phenethyl alcohol) (Supplementary Fig. 1). For behavioral testing outside of the scanner, perceptually similar odor isomers,  $\alpha$  and  $\beta$  pinene, were used in an olfactory three-way forced-choice “triangle” task. Odors were diluted in mineral oil or diethyl phthalate and matched for perceptual intensity.

### **Taste and flavor stimuli**

Taste solutions were made with ACS reagent-grade NaCl and sucrose dissolved in deionized double-distilled water (3D-H<sub>2</sub>O). Tastant dilution series were prepared in fifth-log steps, from  $6.3 \times 10^2$  M to  $4.0 \times 10^{-4}$  M. For retronasal olfactory testing, ethyl butyrate (grape-like flavor) was diluted with 3D-H<sub>2</sub>O and presented at  $1 \times 10^{-5}$  concentration.

### **Behavioral measures**

On days 0, 7, and 14, we tested subjects on five different olfactory measures. (1) Ratings of odor intensity, valence, and familiarity ratings, and pair-wise ratings of odor quality

similarity<sup>8</sup>, were collected for the four odorants used in the fMRI assessment of categorical perception. (2–3) The Sniffin' Sticks Test (Burghart) and the UPSIT (Sensonics) are established standardized measures of odor detection threshold and odor identification, respectively<sup>53,54</sup>. (4) A “triangular” odor discrimination task<sup>7</sup> was performed to test for changes in the ability to discriminate  $\alpha$  and  $\beta$  pinene. (5) Another triangular test was conducted to assess detection of a retronasally delivered odor (ethyl butyrate) from distilled water.

### Non-olfactory behavioral measures

(1) Taste detection thresholds for NaCl and sucrose were based on a criterion of five consecutive correct choices. On each trial, two transfer pipettes were presented, one containing water only, and the other containing salt (or sugar) diluted in water. Subjects sipped from each pipette and indicated which one contained a taste other than water. Each trial was followed by a water rinse, with the next trial ~15 s later<sup>55</sup>. (2) Taste discrimination ability was measured via a three-way forced-choice “triangle” test using NaCl and sucrose solutions at peri-level thresholds of detection (established for each subject on day 0 of baseline testing). (3) Two-point tactile discrimination of the left index finger was measured using paper clips carefully calibrated for points distanced 1 mm to 6 mm<sup>56</sup>. (4) The Benton line-orientation judgment task was used to characterize visuospatial acuity<sup>57</sup>. Note, only subjects who completed a given task on all three testing days were included in that analysis (Table 1).

### Odorant delivery

During behavioral testing, odors were delivered to subjects in opaque amber 30-mL sized glass bottles containing 5-mL solutions of odorants. During fMRI scanning, odorants were delivered using an MRI-compatible computer-controlled olfactometer (air flow, 2.5 L/min), as previously described in our prior studies<sup>58</sup>.

### fMRI procedure

Subjects participated in two tasks during fMRI scanning, conducted across all imaging days. Odorants were delivered using a computer-controlled olfactometer. Sniffing was monitored using respiratory effort bands placed around the chest and abdomen. Subject-specific sniff waveforms were baseline-corrected by subtracting the mean activity in the 500ms preceding sniff onset. Inspiratory volumes and durations for each odor condition were then averaged across trials and subjects.

### fMRI experiment 1

A basic odor detection task was conducted to assess whether mean levels of odor-evoked fMRI activity varied across baseline, post-deprivation, and recovery. On each trial subjects were presented with a visual sniff cue, prompting them to sniff and to indicate with a button press whether they smelled an odor or not (Fig. 1b). The stimulus-onset asynchrony (SOA) between trials was 12 s. Each odorant was presented four times, and odorless air trials were presented 16 times (i.e., 50% of all trials), for an experimental length of ~6.4 minutes.

## fMRI experiment 2

Subjects underwent a second fMRI task (Fig. 1b) designed to assess the multi-voxel pattern integrity of odor quality coding following deprivation. The task was divided into four 10-minute runs, during which time the four odorants and odorless air were each presented 8 times. Odor stimuli were presented for 3 s, with a 15-s SOA. Each session was separated by 90 s. This scanning session lasted ~46 minutes.

## fMRI data acquisition

Gradient-echo T2-weighted echoplanar images (EPI) were acquired with blood oxygen level-dependent (BOLD) contrast on a Siemens Trio 3T MRI scanner, using either a 32-channel ( $n = 9$ ) or a 12-channel ( $n = 2$ ) head coil. Imaging parameters were: TR, 1.51 s; TE, 20 ms; slice thickness, 2 mm; gap, 1 mm; matrix size, 128×120 voxels; field-of-view, 220×206 mm; in-plane resolution, 1.72×1.72 mm. Image acquisition was tilted at 30° from horizontal to reduce susceptibility artifact in olfactory regions. A 1-mm isotropic T1-weighted MPRAGE structural MRI scan was obtained to aid in defining anatomical regions of interest (ROIs).

## fMRI pre-processing

fMRI data were pre-processed with SPM5 software ([www.fil.ion.ucl.ac.uk/spm/](http://www.fil.ion.ucl.ac.uk/spm/)). Images were spatially realigned to the first volume of the first session (pre-deprivation). For univariate fMRI analysis, this was followed by spatial normalization to a standard EPI template, and spatial smoothing (6-mm kernel) to account for residual inter-subject differences. For multivariate fMRI analysis, there were no subsequent preprocessing steps beyond spatial realignment, to preserve the voxel-wise fidelity of the fMRI signal.

## Univariate fMRI models

The pre-processed fMRI data from the odor detection task (fMRI experiment 1) were analyzed using an event-related general linear model (GLM), created by modeling onset times for the odor conditions (pooled across all four odorants) and for the odorless air condition with stick (delta) functions, convolved with a standard hemodynamic response function (HRF) to generate two regressors of interest for baseline, post-deprivation, and recovery sessions. Models included six head movement-related regressors per fMRI session, obtained from the spatial realignment step. Temporal auto-correlations were adjusted using an auto-regressive (AR[1]) process. A 128-s high-pass filter was used to remove signal drifts. Voxel-wise, condition-specific beta values were then estimated for odor and no-odor conditions.

Subsequently, a flexible-factorial model was used to investigate effects at the group (random effects) level. Subject-specific parameter estimates for the six conditions were modeled in SPM5 using a two-by-three repeated-measures ANOVA, with the factors “odor presence” (yes/no) and “time” (baseline/post-deprivation/recovery), with non-sphericity correction. An omnibus F-contrast tested for odor-evoked mean fMRI activity changes across time (Supplementary Table 1). Significance was set at  $P < 0.05$  whole-brain corrected for multiple comparisons using the false-discovery-rate (FDR) option in SPM5.

Conjunction “null” analyses were conducted in SPM5<sup>32,33</sup> to confirm whether brain regions showed deprivation-selective changes that recovered to baseline levels. Conjunction contrasts of interest were [post-deprivation>baseline] & [post-deprivation>recovery], as well as the converse conjunction, [baseline>post-deprivation] & [recovery>post-deprivation]. Significance for each contrast was set at  $p < 0.005$  uncorrected (corresponding to a conjoined  $p < 0.000025$ ), delimited to activations observed within the omnibus F-test inclusively masked at  $p < 0.05$  uncorrected.

To assess the statistical robustness of the conjunction effects, we conducted a “leave-one-subject-out” analysis<sup>32</sup> to maintain independence of voxel identification and small-volume correction<sup>35</sup>. A group-level model was specified, identical to the above procedures, except that only nine of the ten subjects was included, with one subject left out. Peak coordinates from the conjunction analyses were identified from this nine-subject model, and then used as SVC (6-mm radius) for the observed fMRI activations from the conjunction analysis of the tenth (left-out) subject. This procedure was iteratively repeated for all ten subjects. Beta values were converted to BOLD percent signal change and tested for differences over time. Conjunction analysis of the APC was based on regions centered at  $-30, 4, -16$ , and  $-20, 4, -12$  (6-mm radius), derived from a prior study<sup>8</sup>. SVC peak coordinates are reported in Supplementary Table 2.

### Multivariate pattern analysis

We used a multivariate approach to analyze neuroimaging data from fMRI experiment 2 to evaluate categorical representations of odor quality. Multi-voxel ensembles of odor-evoked fMRI activity patterns were extracted from ROIs in APC, PPC, and OFC, defined *a priori* on the basis of prior imaging studies<sup>7,8,36,59</sup>. Anatomical ROIs were manually drawn on each subject’s T1-weighted MRI scan using MRIcroN software (<http://www.micron.com/>). APC and PPC were drawn with reference to a human brain atlas<sup>60</sup>, whereas delineation of OFC was guided by an olfactory fMRI meta-analysis<sup>59</sup>.

For each subject, a GLM was specified for each scanning session from the spatially aligned, but un-normalized, unsmoothed fMRI data. For each session, the four runs were sorted into even and odd halves. For each half, five vectors of onset times were generated for the four odor conditions and the odorless air condition (correct trials only). These regressors were convolved with the HRF; all other modeling steps were identical to those described for univariate analysis. Following model estimation, beta values were extracted from all voxels within each ROI and assembled into condition-specific linear vectors of ensemble activity.

Ensemble activity patterns were analyzed in two ways. First, we examined pattern correlations between odors belonging to the same category. We constrained the set of voxels within a given ROI to those that showed quality coding selectivity. This procedure utilized an independent voxel selection method<sup>7,36</sup>, in which the [odor–air] contrast from the pre-deprivation scan in fMRI experiment 1 was used to rank voxels according to their T-value. Correlation differences between quality-related and quality-unrelated odorant pairs were computed iteratively for increasing numbers of voxels (by T-value rank); that set of voxels exhibiting maximal discriminative validity in the baseline (pre-deprivation) period was then used to *independently compute* correlation differences for post-deprivation and recovery

periods<sup>7</sup>. A similar approach was used to select voxels based on functional-group discriminability in the baseline scanning session, to assess changes in ensemble coding of this molecular parameter.

Second, we computed pattern correlations between all odorant pairs for each ROI, to assess general changes in odor-evoked ensemble activity. Pattern correlations between odd and even ensembles of odor vs. odorless air were also calculated as a control measure of pattern overlap arising from sniffing per se. Correlation differences between odor:odor and odor:air were estimated for each subject separately for baseline, post-deprivation, and recovery.

### Statistical analyses

Results are shown as mean  $\pm$  s.e.m. for participants and conditions. To test for group differences in pattern correlations across time, we performed repeated-measures ANOVAs, with follow-up post-hoc Student T-tests where appropriate. For correlation analyses of behavioral and neuroimaging data, Spearman's rank correlation coefficients were calculated. Statistical inference was set at a significance of  $P < 0.05$  unless otherwise stated.

### Supplementary Material

Refer to Web version on PubMed Central for supplementary material.

### Acknowledgments

The authors would like to thank M. Cahill for assistance in nasal endoscopy and acoustic rhinometry measurements. N. Sandalow and K. Phillips for technical assistance and data collection, and International Flavors and Fragrances Inc. and S. Warrenburg for providing the odorless grade solvents. This work was supported by Northwestern Institutional Predoctoral Training Awards to K.N.W. (#T32NS047987) and to J.D.H. (#T32 MH067564), grants #R01DC010014 and #K08DC007653 from the National Institute on Deafness and Other Communication Disorders to J.A.G., and NIH grant #M01-RR00048 from the National Center for Research Resources to Northwestern University Feinberg School of Medicine.

### References

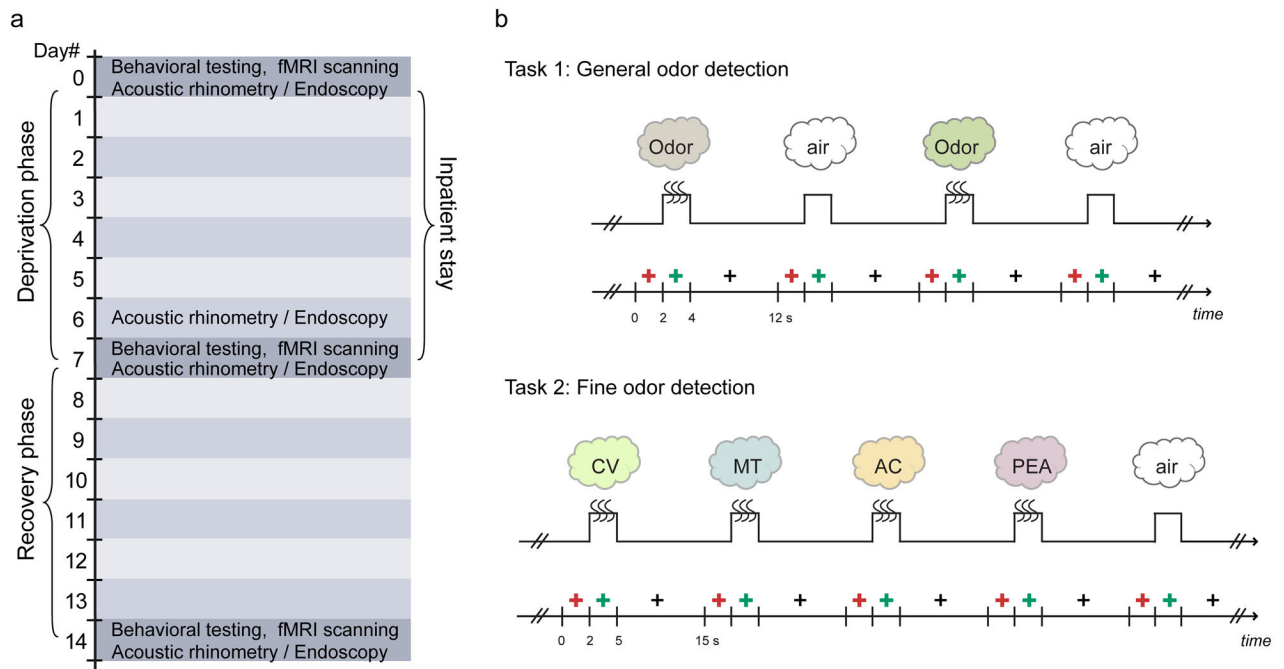
1. Wiesel TN, Hubel DH. Single-Cell Responses in Striate Cortex of Kittens Deprived of Vision in One Eye. *J Neurophysiol.* 1963; 26:1003–17. [PubMed: 14084161]
2. Van der Loos H, Woolsey TA. Somatosensory cortex: structural alterations following early injury to sense organs. *Science.* 1973; 179:395–8. [PubMed: 4682966]
3. Merzenich MM, et al. Somatosensory cortical map changes following digit amputation in adult monkeys. *J Comp Neurol.* 1984; 224:591–605. [PubMed: 6725633]
4. Hubel DH, Wiesel TN. The period of susceptibility to the physiological effects of unilateral eye closure in kittens. *J Physiol.* 1970; 206:419–36. [PubMed: 5498493]
5. Linkenhoker BA, Knudsen EI. Incremental training increases the plasticity of the auditory space map in adult barn owls. *Nature.* 2002; 419:293–6. [PubMed: 12239566]
6. Scheiman MM, et al. Randomized trial of treatment of amblyopia in children aged 7 to 17 years. *Arch Ophthalmol.* 2005; 123:437–47. [PubMed: 15824215]
7. Li W, Howard JD, Parrish TB, Gottfried JA. Aversive learning enhances perceptual and cortical discrimination of indiscriminable odor cues. *Science.* 2008; 319:1842–5. [PubMed: 18369149]
8. Li W, Luxenberg E, Parrish T, Gottfried JA. Learning to smell the roses: experience-dependent neural plasticity in human piriform and orbitofrontal cortices. *Neuron.* 2006; 52:1097–108. [PubMed: 17178411]



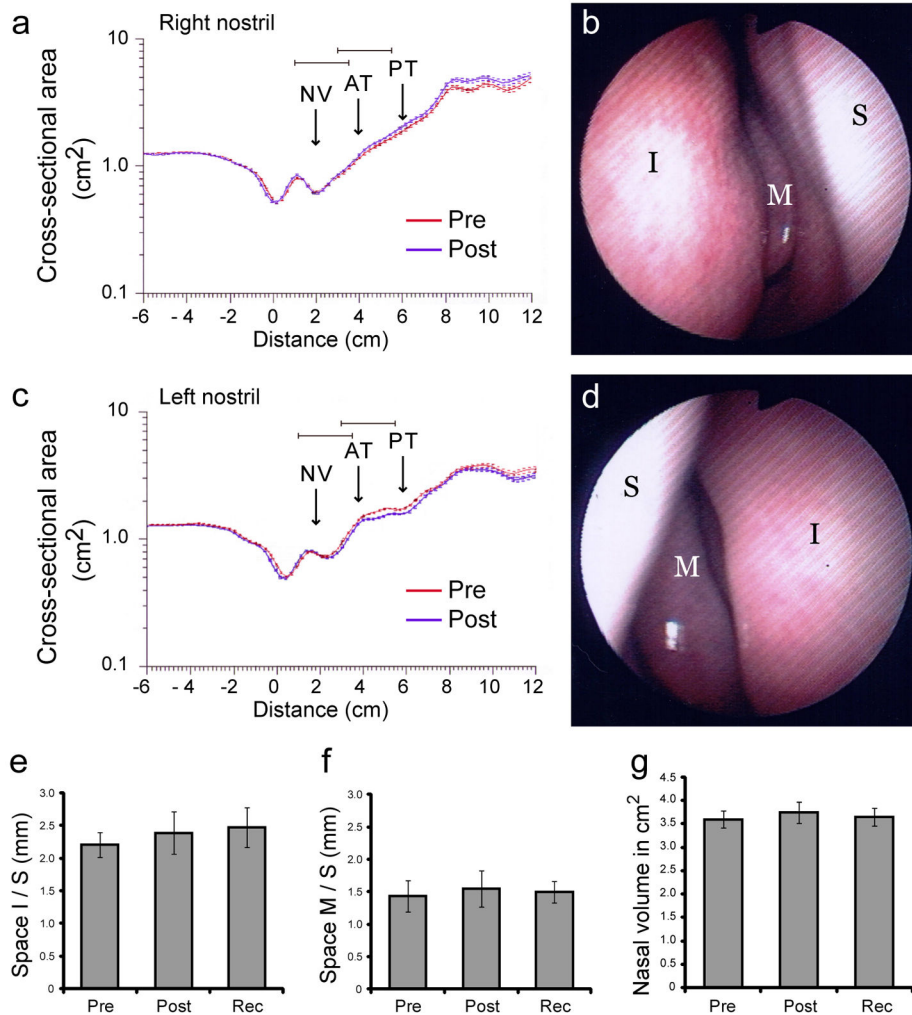
9. Hofer SB, Mrcsic-Flogel TD, Bonhoeffer T, Hubener M. Prior experience enhances plasticity in adult visual cortex. *Nat Neurosci.* 2006; 9:127–32. [PubMed: 16327785]
10. Wilson DA, Wood JG. Functional consequences of unilateral olfactory deprivation: time-course and age sensitivity. *Neuroscience.* 1992; 49:183–92. [PubMed: 1357586]
11. Maruniak JA, Taylor JA, Henegar JR, Williams MB. Unilateral naris closure in adult mice: atrophy of the deprived-side olfactory bulbs. *Brain Res Dev Brain Res.* 1989; 47:27–33. [PubMed: 2736765]
12. Corotto FS, Henegar JR, Maruniak JA. Odor deprivation leads to reduced neurogenesis and reduced neuronal survival in the olfactory bulb of the adult mouse. *Neuroscience.* 1994; 61:739–44. [PubMed: 7838373]
13. Best AR, Wilson DA. A postnatal sensitive period for plasticity of cortical afferents but not cortical association fibers in rat piriform cortex. *Brain Res.* 2003; 961:81–7. [PubMed: 12535779]
14. Livneh Y, Mizrahi A. Experience-dependent plasticity of mature adult-born neurons. *Nat Neurosci.* 2011; 15:26–8. [PubMed: 22081159]
15. Boroojerdi B, et al. Enhanced excitability of the human visual cortex induced by short-term light deprivation. *Cereb Cortex.* 2000; 10:529–34. [PubMed: 10847602]
16. Pitskel NB, Merabet LB, Ramos-Estebanez C, Kauffman T, Pascual-Leone A. Time-dependent changes in cortical excitability after prolonged visual deprivation. *Neuroreport.* 2007; 18:1703–7. [PubMed: 17921872]
17. Pantev C, Wollbrink A, Roberts LE, Engelien A, Lutkenhoner B. Short-term plasticity of the human auditory cortex. *Brain Res.* 1999; 842:192–9. [PubMed: 10526109]
18. Rossini PM, et al. Short-term brain ‘plasticity’ in humans: transient finger representation changes in sensory cortex somatotopy following ischemic anesthesia. *Brain Res.* 1994; 642:169–77. [PubMed: 8032877]
19. Sireteanu R, Oertel V, Mohr H, Linden D, Singer W. Graphical illustration and functional neuroimaging of visual hallucinations during prolonged blindfolding: a comparison to visual imagery. *Perception.* 2008; 37:1805–21. [PubMed: 19227374]
20. Merabet LB, Pascual-Leone A. Neural reorganization following sensory loss: the opportunity of change. *Nat Rev Neurosci.* 2010; 11:44–52. [PubMed: 19935836]
21. Lledo PM, Saghatelian A. Integrating new neurons into the adult olfactory bulb: joining the network, life-death decisions, and the effects of sensory experience. *Trends Neurosci.* 2005; 28:248–54. [PubMed: 15866199]
22. Graziadei PP, Graziadei GA. Neurogenesis and neuron regeneration in the olfactory system of mammals. I. Morphological aspects of differentiation and structural organization of the olfactory sensory neurons. *J Neurocytol.* 1979; 8:1–18. [PubMed: 438867]
23. Weiler E, Farbman AI. Proliferation in the rat olfactory epithelium: age-dependent changes. *J Neurosci.* 1997; 17:3610–22. [PubMed: 9133384]
24. Angely CJ, Coppola DM. How does long-term odor deprivation affect the olfactory capacity of adult mice? *Behav Brain Funct.* 2010; 6:26. [PubMed: 20500833]
25. Guthrie KM, Wilson DA, Leon M. Early unilateral deprivation modifies olfactory bulb function. *J Neurosci.* 1990; 10:3402–12. [PubMed: 1976769]
26. Hunt NL, Slotnick BM. Functional-Capacity of the Rat Olfactory-Bulb after Neonatal Naris Occlusion. *Chemical Senses.* 1991; 16:131–142.
27. Kim HH, Puche AC, Margolis FL. Odorant deprivation reversibly modulates transsynaptic changes in the NR2B-mediated CREB pathway in mouse piriform cortex. *J Neurosci.* 2006; 26:9548–59. [PubMed: 16971539]
28. Wilson DA, Best AR, Brunjes PC. Trans-neuronal modification of anterior piriform cortical circuitry in the rat. *Brain Res.* 2000; 853:317–22. [PubMed: 10640629]
29. Wilson DA, Sullivan RM. The D2 antagonist spiperone mimics the effects of olfactory deprivation on mitral/tufted cell odor response patterns. *J Neurosci.* 1995; 15:5574–81. [PubMed: 7643202]
30. Brunjes PC, Borrer MJ. Unilateral odor deprivation: differential effects due to time of treatment. *Brain Res Bull.* 1983; 11:501–3. [PubMed: 6667380]

31. Luskin MB, Price JL. The topographic organization of associational fibers of the olfactory system in the rat, including centrifugal fibers to the olfactory bulb. *J Comp Neurol*. 1983; 216:264–91. [PubMed: 6306065]
32. Friston KJ, Penny WD, Glaser DE. Conjunction revisited. *Neuroimage*. 2005; 25:661–7. [PubMed: 15808967]
33. Nichols T, Brett M, Andersson J, Wager T, Poline JB. Valid conjunction inference with the minimum statistic. *Neuroimage*. 2005; 25:653–60. [PubMed: 15808966]
34. Esterman M, Tamber-Rosenau BJ, Chiu YC, Yantis S. Avoiding non-independence in fMRI data analysis: leave one subject out. *Neuroimage*. 2010; 50:572–6. [PubMed: 20006712]
35. Worsley KJ, et al. A unified statistical approach for determining significant signals in images of cerebral activation. *Hum Brain Mapp*. 1996; 4:58–73. [PubMed: 20408186]
36. Howard JD, Plailly J, Grueschow M, Haynes JD, Gottfried JA. Odor quality coding and categorization in human posterior piriform cortex. *Nat Neurosci*. 2009; 12:932–8. [PubMed: 19483688]
37. Rolls ET, Grabenhorst F, Parris BA. Neural systems underlying decisions about affective odors. *J Cogn Neurosci*. 2010; 22:1069–82. [PubMed: 19320548]
38. Zelano C, Mohanty A, Gottfried JA. Olfactory predictive codes and stimulus templates in piriform cortex. *Neuron*. 2011; 72:178–87. [PubMed: 21982378]
39. Illig KR. Projections from orbitofrontal cortex to anterior piriform cortex in the rat suggest a role in olfactory information processing. *J Comp Neurol*. 2005; 488:224–31. [PubMed: 15924345]
40. Cohen Y, Reuveni I, Barkai E, Maroun M. Olfactory learning-induced long-lasting enhancement of descending and ascending synaptic transmission to the piriform cortex. *J Neurosci*. 2008; 28:6664–9. [PubMed: 18579740]
41. Carmichael ST, Clugnet MC, Price JL. Central olfactory connections in the macaque monkey. *J Comp Neurol*. 1994; 346:403–34. [PubMed: 7527806]
42. Schoenbaum G, Eichenbaum H. Information coding in the rodent prefrontal cortex. II. Ensemble activity in orbitofrontal cortex. *J Neurophysiol*. 1995; 74:751–62. [PubMed: 7472379]
43. Critchley HD, Rolls ET. Olfactory neuronal responses in the primate orbitofrontal cortex: analysis in an olfactory discrimination task. *J Neurophysiol*. 1996; 75:1659–72. [PubMed: 8727404]
44. Roesch MR, Stalnaker TA, Schoenbaum G. Associative encoding in anterior piriform cortex versus orbitofrontal cortex during odor discrimination and reversal learning. *Cereb Cortex*. 2007; 17:643–52. [PubMed: 16699083]
45. van Wingerden M, Vinck M, Lankelma J, Pennartz CM. Theta-band phase locking of orbitofrontal neurons during reward expectancy. *J Neurosci*. 2010; 30:7078–87. [PubMed: 20484650]
46. Plailly J, Howard JD, Gitelman DR, Gottfried JA. Attention to odor modulates thalamocortical connectivity in the human brain. *J Neurosci*. 2008; 28:5257–67. [PubMed: 18480282]
47. Waggener CT, Coppola DM. Naris occlusion alters the electro-olfactogram: evidence for compensatory plasticity in the olfactory system. *Neurosci Lett*. 2007; 427:112–6. [PubMed: 17931777]
48. Korol DL, Brunjes PC. Rapid changes in 2-deoxyglucose uptake and amino acid incorporation following unilateral odor deprivation: a laminar analysis. *Brain Res Dev Brain Res*. 1990; 52:75–84. [PubMed: 2331802]
49. Philpot BD, Foster TC, Brunjes PC. Mitral/tufted cell activity is attenuated and becomes uncoupled from respiration following naris closure. *J Neurobiol*. 1997; 33:374–86. [PubMed: 9322155]
50. Holbrook EH, Leopold DA. An updated review of clinical olfaction. *Curr Opin Otolaryngol Head Neck Surg*. 2006; 14:23–8. [PubMed: 16467634]
51. Hilberg O. Objective measurement of nasal airway dimensions using acoustic rhinometry: methodological and clinical aspects. *Allergy*. 2002; 57 (Suppl 70):5–39. [PubMed: 11990714]
52. Hasegawa M, Kern EB. The human nasal cycle. *Mayo Clin Proc*. 1977; 52:28–34. [PubMed: 609283]
53. Doty RL, Shaman P, Kimmelman CP, Dann MS. University of Pennsylvania Smell Identification Test: a rapid quantitative olfactory function test for the clinic. *Laryngoscope*. 1984; 94:176–8. [PubMed: 6694486]

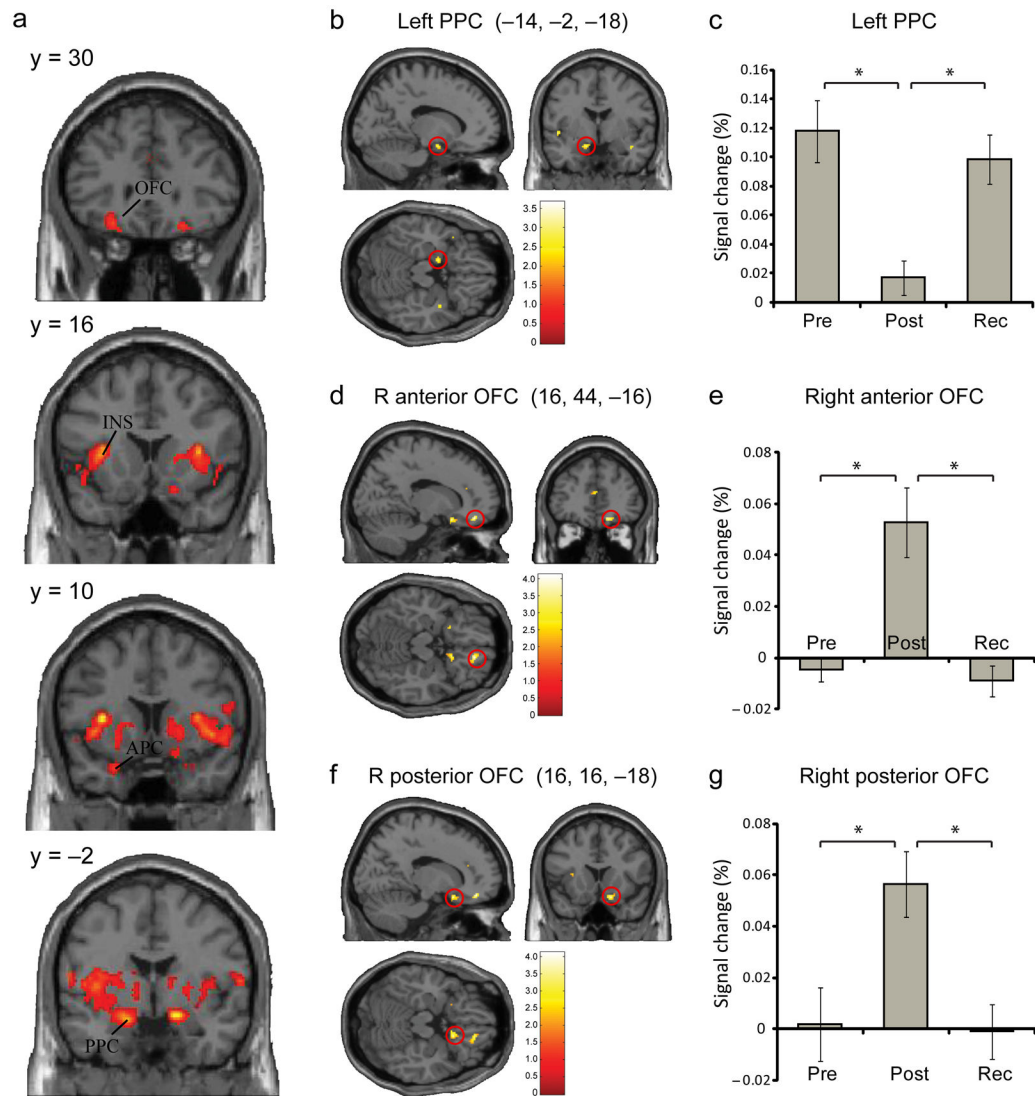
54. Hummel T, Sekinger B, Wolf SR, Pauli E, Kobal G. 'Sniffin' sticks': olfactory performance assessed by the combined testing of odor identification, odor discrimination and olfactory threshold. *Chem Senses*. 1997; 22:39–52. [PubMed: 9056084]
55. Bartoshuk LM. The psychophysics of taste. *Am J Clin Nutr*. 1978; 31:1068–77. [PubMed: 352127]
56. Finnell JT, Knopp R, Johnson P, Holland PC, Schubert W. A calibrated paper clip is a reliable measure of two-point discrimination. *Acad Emerg Med*. 2004; 11:710–4. [PubMed: 15175216]
57. Benton AL, Varney NR, Hamsher KD. Visuospatial judgment. A clinical test. *Arch Neurol*. 1978; 35:364–7. [PubMed: 655909]
58. Gottfried JA, Deichmann R, Winston JS, Dolan RJ. Functional heterogeneity in human olfactory cortex: an event-related functional magnetic resonance imaging study. *J Neurosci*. 2002; 22:10819–28. [PubMed: 12486175]
59. Gottfried JA, Zald DH. On the scent of human olfactory orbitofrontal cortex: meta-analysis and comparison to non-human primates. *Brain Res Brain Res Rev*. 2005; 50:287–304. [PubMed: 16213593]
60. Mai, JK.; Assheuer, J.; Paxinos, G. Atlas of the human brain. Vol. viii. Academic Press; San Diego: 1997. p. 328

**Fig 1.**

Experimental design. **(a)** Timeline of the 14-day experiment requiring laboratory visits at day 0 (baseline), day 7, and day 14. Subjects were admitted for a 7-day inpatient stay during the deprivation phase, and were then discharged and allowed a 7-day recovery period before returning for a final testing session. **(b)** Schematic diagram of the fMRI experiments. Two seconds prior to odor delivery, a red cross-hair appeared on screen to indicate that an odor was forthcoming. A change in the color of the cross-hair from red to green served as the sniff cue, prompting the subject to make a sniff, and either an odorant (or odorless air) was presented via a computer-controlled olfactometer to the subject's nose. At the offset of odor presentation, a black cross-hair appeared and subjects responded by pressing a button to indicate whether they detected an odor or not. CV, (*R*)-carvone; MT, L-menthol; AC, acetophenone; PEA, phenethyl alcohol.

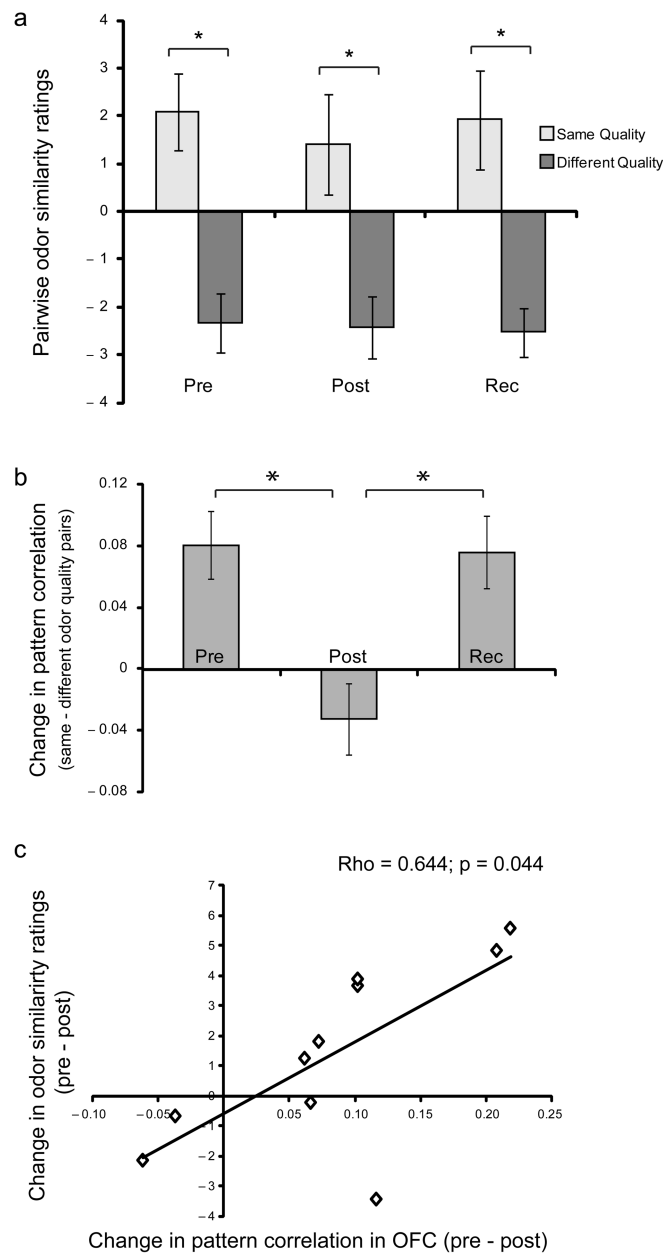


**Fig 2.** Rhinological data and nasal endoscopic measurements. (a–d) Data from one representative subject. Acoustic rhinometry of the right (a) and left (c) internal nasal cavities revealed considerable uniformity in airway area and volume from pre to post-deprivation. Each rhinogram trace is an average of 10 consecutive measurements and depicts cross-sectional area as a function of distance from nostril entrance (at 0cm). Arrows mark approximate regions of nasal valve (NV), anterior parts of inferior and middle turbinates (AT), and mid-posterior part of middle turbinate (PT). Nasal endoscopy of the right (b) and left (d) nasal cavities immediately after deprivation revealed healthy tissue without rhinitis or edema. (e–g) Group-averaged endoscopic measurements (mean  $\pm$  s.e.m.) from 11 subjects show that odor deprivation had no effect on the average space between (e) the inferior turbinate and septum and (f) between the middle turbinate and septum from 11 subjects as observed during nasal endoscopy observation on each testing session. (g) Group-averaged acoustic rhinometric measurements of internal nasal volume (between 1–5cm from the nostril entrance; average of 10 consecutive measurements per subject) also show no significant differences across testing days. I, inferior turbinate; M, middle turbinate; S, septum. Measurements shown in e–g were averaged across both nostrils.

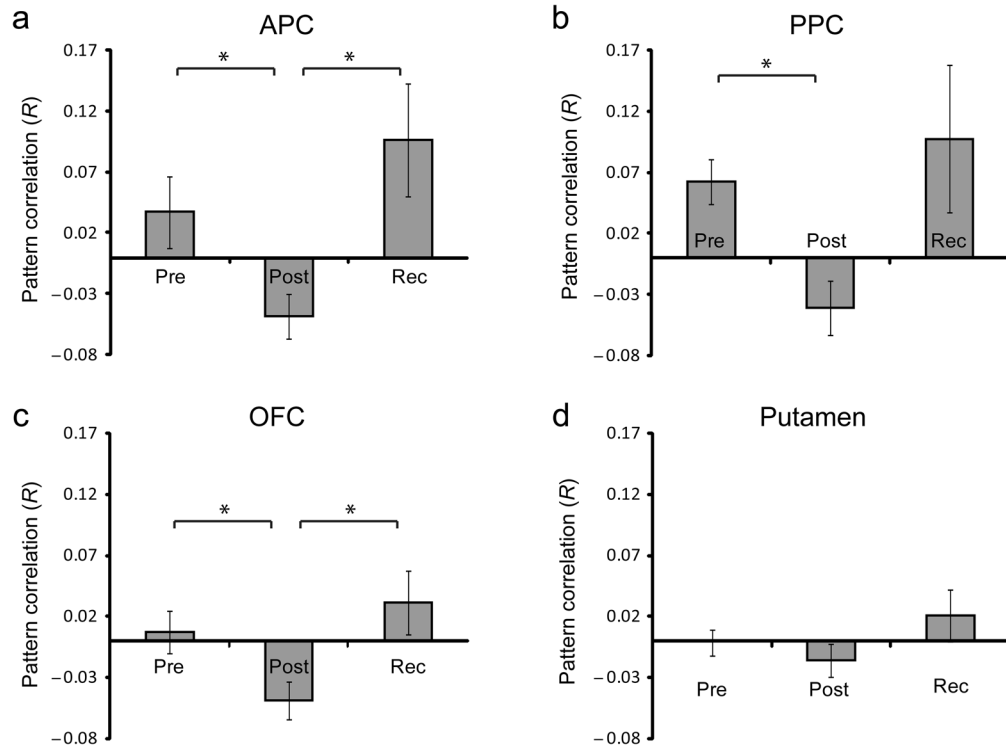


**Fig 3.** fMRI Experiment 1: univariate fMRI results. **(a)** Areas showing significant changes in odor-evoked activity across the three testing sessions included bilateral anterior piriform cortex (APC), posterior piriform cortex (PPC), orbitofrontal cortex (OFC), and insula (INS) (omnibus F-contrast; display threshold,  $p < 0.001$ ). **(b,c)** An fMRI conjunction analysis revealed a deprivation-selective decrement of odor-evoked activity in the left PPC that returned to baseline levels at recovery. **(d–g)** The reverse conjunction analysis showed a deprivation-selective increment in the right anterior and posterior OFC, opposite in response direction to PPC. Plots of percent signal change in panels **c**, **e**, and **g** are based on the mean of single-subject beta values (mean  $\pm$  s.e.m.) extracted from PPC and OFC using a leave-one-subject-out cross-validation analysis. (\*) denotes statistical significance of  $p < 0.05$  (small-volume corrected).





**Fig 4.** fMRI Experiment 2: behavioral and multivariate fMRI results. **(a)** Across all three testing sessions, subjects rated odorant pairs belonging to the same (vs. different) perceptual category as significantly more similar. **(b)** Spatial ensemble patterns of fMRI activity (mean  $\pm$  s.e.m.) in OFC showed significantly more overlap between categorically similar (vs. different) odorants at pre-deprivation. Following deprivation, these pattern differences significantly diminished, returning to baseline levels after recovery. **(c)** A scatterplot highlights the correlation between the magnitude of quality-related pattern decorrelation in the OFC and subject-wise perceptual changes in odor similarity ratings, from pre- to post-deprivation. Each diamond represents one subject. \*,  $p < 0.05$ .

**Fig 5.**

General deprivation-related changes in fMRI ensemble activity (fMRI Experiment 2). Pattern correlations of odor-evoked fMRI ensemble activity (mean  $\pm$  s.e.m.) were based on anatomically defined, functionally unrestricted ROIs, and were computed across all odorant pairs, irrespective of pairwise perceptual or molecular similarity. Deprivation-related pattern decorrelations were identified in APC, PPC, and OFC, but not putamen, a non-olfactory control ROI. \*,  $p < 0.05$ . Rec, recovery.

**Table 1**

Behavioral performance on olfactory and non-olfactory tasks over baseline (day 0), post-deprivation (day 7), and recovery (day 14) sessions. Scores presented as means  $\pm$  s.e.m. Note that due to the time-sensitive nature of this study, the number of tasks administered, and unpredictable technical difficulties at the MRI scanner, not all subjects completed all of the tasks.

<b>Task</b>	<b>Baseline</b>	<b>Post-depriv.</b>	<b>Recovery</b>	<b>#Sub</b>
Sniffin' Sticks (odor detection threshold)	10.23 $\pm$ 1.05	9.87 $\pm$ 0.78	9.92 $\pm$ 1.03	n = 13
UPSIT (odor identification)	35.00 $\pm$ 0.59	36.29 $\pm$ 0.80	35.79 $\pm$ 0.73	n = 14
Odor Similarity Ratings (odor quality perception)	4.81 $\pm$ 0.73	3.60 $\pm$ 1.13	4.08 $\pm$ 1.30	n = 13
Pinene Triangle Test (fine odor discrimination)	7.45 $\pm$ 0.81	6.91 $\pm$ 0.90	6.64 $\pm$ 0.88	n = 11
NaCl Detection Threshold	6.82 $\pm$ 0.53	6.60 $\pm$ 0.45	7.40 $\pm$ 0.44	n = 10
Sucrose Detection Threshold	5.70 $\pm$ 0.95	6.90 $\pm$ 0.80	7.40 $\pm$ 0.94	n = 10
NaCl Sucrose Triangle Task (taste discrimination)	7.27 $\pm$ 0.69	7.36 $\pm$ 0.74	8.45 $\pm$ 0.67	n = 11
Retronasal Flavor Detection	9.82 $\pm$ 0.57	9.00 $\pm$ 0.82	8.73 $\pm$ 0.75	n = 11
Visual Orientation Judgment	26.64 $\pm$ 0.70	27.71 $\pm$ 0.67	27.85 $\pm$ 0.55	n = 14
2-pt Tactile Discrimination	2.45 $\pm$ 0.12	2.34 $\pm$ 0.12	2.49 $\pm$ 0.10	n = 14